Triphenylamine-based allylidenemalonitrile chromophores: Synthesis, photophysical and second-order nonlinear optical properties.

Emine Çatal,[a] Ergin Keleş,[a] Nurgül Seferoğlu,[b] Sylvain Achelle,*[c] Alberto Barsella,[d] Françoise Robin-le Guen[c] and Zeynel Seferoğlu*[a]

[a] Gazi University, Department of Chemistry, 06500, Ankara

[b] Gazi University, Advanced Technology Department, Inst. Sci. & Technol., Ankara, Turkey

[c] Univ Rennes, CNRS, Institut des Sciences Chimiques de Rennes - UMR6226, F 35000 Rennes, France

[d] Département d'Optique Ultra-Rapide et Nanophotonique, IPCMS, UMR CNRS 7504, Université de Strasbourg, 23 Rue du Loess, BP 43, 67034 Strasbourg Cedex 2, France

Graphical abstract

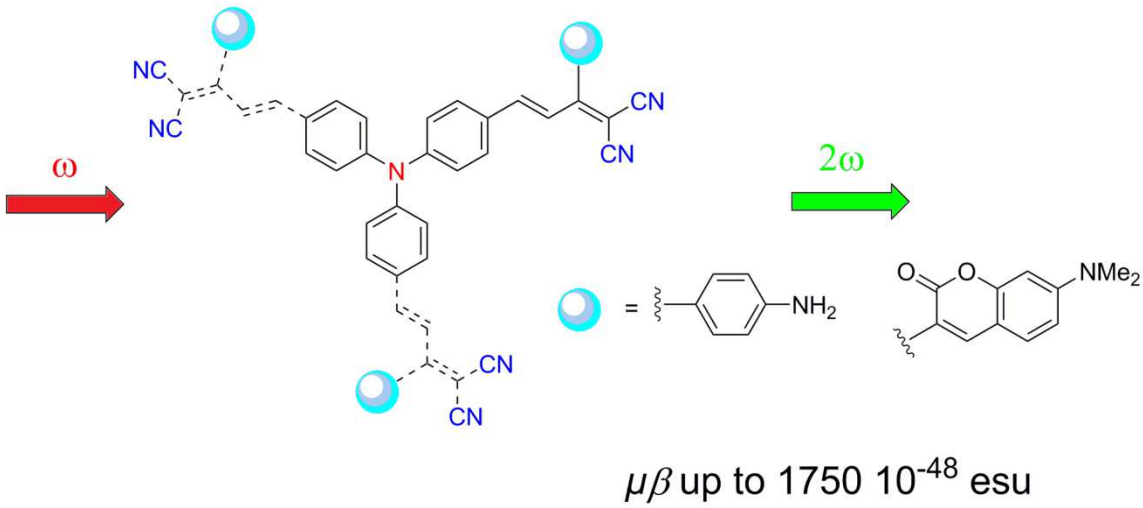

Abstract

A series of chromophores based on a mono- di- of tri-substituted triphenylamine core and allylidenemalonitrile fragments has been designed. The linear and second order nonlinear optical properties as well as thermal stability of the chromophores have been studied

experimentally. Structure-properties relationships, in term of branching effect on the triphenylamine core and the influence of aniline/coumarin part on the photophysical properties and NLO response have been highlighted. Experimental results have been rationalized by theoretical calculations.

Introduction

Nonlinear optic (NLO) has been subject to intensive research since the development of lasers. Under high intensity electromagnetic excitation, NLO-chromophores undergo modification of their electronic structure leading to modification of their optical properties.[1] Second order NLO-chromophores exhibit high first order hyperpolarizability β and have been used for the generation of new frequencies of coherent light, electrooptic modulation and photonic switching with applications such as the generation of a green laser from a red source, the terahertz wave generation for telecommunication and the second/third harmonic microscopy.[2] Second order NLO chromophores are generally inorganic materials. Nevertheless, organic materials offer several advantages such as well-defined and easily tunable structures and large NLO responses. The D-π-A push-pull structure is typical of second order NLO chromophores and the first order hyperpolarizability is closely related to the intramolecular charge transfer (ICT) into the molecule.[3] The NLO properties can be tuned by playing on the donor/acceptor couple[4] or by varying the π-conjugated linker.[5] In addition to the ordinary linear D-π-A systems, quadrupolar (D-(π-A)$_2$ or A-(π-A)$_2$) and octupolar (D-(π-A)$_3$ or A-(π-A)$_3$) structures can be also used for second order NLO properties provided the chromophores are not centrosymetric.[6]

The triphenylamine building block has been extensively used as electron-donating group for push-pull structures. Triphenylamine derivatives with electron-withdrawing substituents are well-known for their high luminescence[7] and two-photon absorption (TPA) properties.[8] The

mono-, di-, and tri- substitution of the triphenylamine core permit to obtain dipolar, quadrupolar and octupolar structures. A significant branching effect has been observed on the TPA properties.[9] Dipolar monosubstituted triphenylamine derivatives have been extensively described as second order NLO chromophores,[10] but quadrupolar and octupolar triphenylamine chromophores have been rarely used in this context.[11]

Recently, allylidenemalonitrile derivatives have been proposed as NLO chromophores.[12] Some of these compounds exhibit high figure of merit.[13]

In this contribution we describe the synthesis of triphenylamine derivatived decorated with one, two or three allylidenemanolonitrile fragments bearing aniline or coumarin groups (Chart 1). Their photophysical and second order NLO properties as well as their thermal stability were also studied. TD-DFT calculations were also performed to gain further insight into the ICT occurring in these structures.

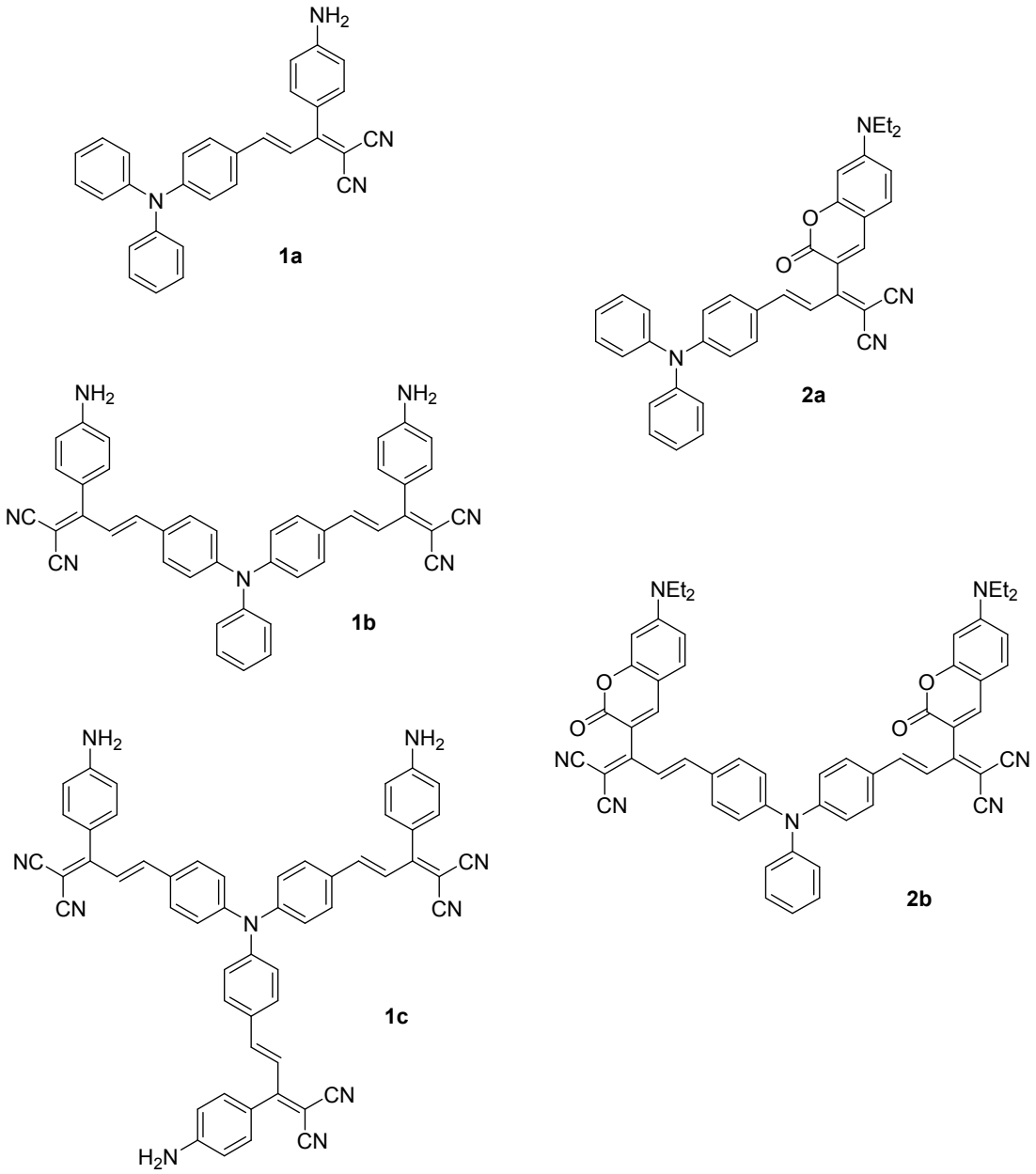

Chart 1: Structure of studied compounds

Results and discussion

Synthesis

Compounds **1** and **2** were obtained with moderate to good yield by condensation of the corresponding ethylidenemalononitrile derivative[14] on mono-, di-or tri-formyltriphenylamine starting material (Scheme 1) according to a procedure developed previously by some of us.[13] It should be noted that due to solubility problem, the synthesis of compound **1c** from tri-

formyltriphenylamine has been performed in MeCN instead of EtOH. The chromophore with three coumarin fragments was not isolated, once again due to solubility reason even when using MeCN as solvent.

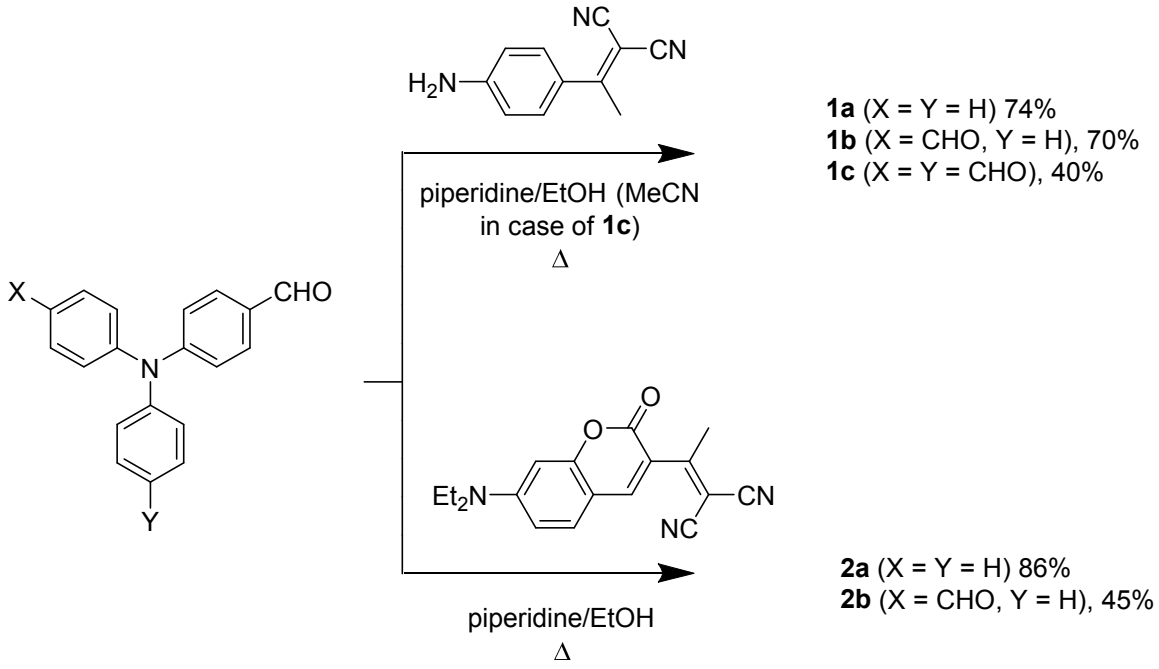

Scheme 1: Synthesis of compounds **1** and **2.**

Linear Optical Properties

The UV-vis and photoluminescence (PL) spectroscopic data for compounds **1** and **2**, measured in chloroform are presented in Table 1 and the normalized spectra are shown in figure 1. The analyses were carried out using low concentration solution ((1.0-2.0) × 10^{-5} M for absorption, (1.0-2.0) × 10^{-6} M for emission). Under these conditions, self absorption effects were not observed.

Table 1. UV-vis and photoluminescence (PL) data in $CHCl_3$ solution.

Compd	λ_{abs} (nm)	ε (mM^{-1} cm^{-1})	λ_{em} (nm)	Φ_F[a]	Stokes shift[b] (cm^{-1})	Brightness[b,c] (mM^{-1} cm^{-1})
1a	304, 490	26.8, 40.0	629	0.16	4510	6.4
1b	451sh, 512	37.8, 54.5	613	0.26	3218	14.2
1c	345, 509	30.4, 59.4	612	0.30	3306	17.8
2a	387, 507	39.2, 86.8	666	0.32	4709	27.7
2b	397, 470	39.1 41.0	654	0.19	5986	7.8

[a]Fluorescence quantum yield (±10%) determined relative to 9,10-bis(phenylethynyl)anthracene in cyclohexane (Φ_F = 1.00) as standard. [b]Calculated using the less energetic absorption band [c]Calculated as the product of ε and Φ_F.

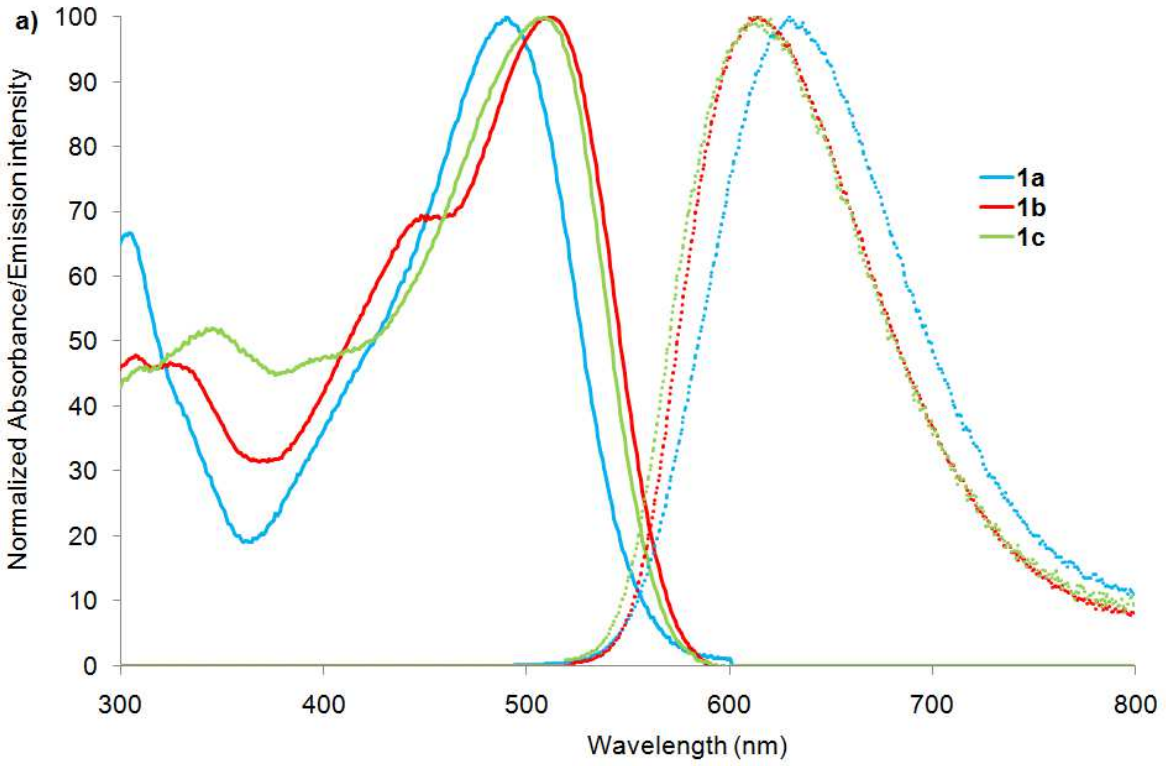

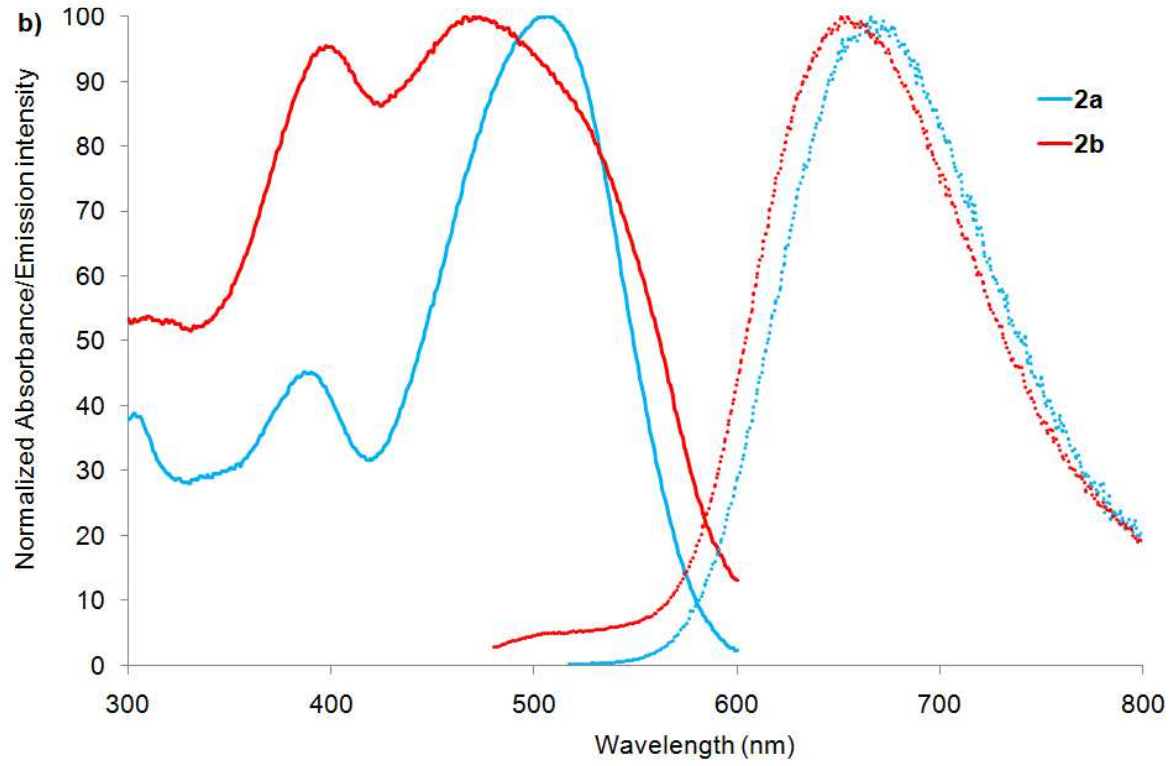

Figure 1. Normalized absorption and emission spectra in $CHCl_3$ of compounds **1** (part a) and **2** (part b)

All the compounds exhibited orange-red emission with quantum yield up to 0.32. For compounds **1**, it appears that the polysubstitution of the triphenylamine core results in blue-shifted emission associated with a significant increase of the quantum yield and of the molar extinction coefficient of the charge transfer absorption band, leading to an enhanced brightness. The emission of compounds **2b** is also blue-shifted in comparison with compound **2a**, in accordance with the observation on other series of triphenylamine derivatives.[7a,9b,15] As far as coumarin (**2**) and aniline (**1**) derivatives are compared, a significant bathochormic shift is observed either in absorption and emission in case of compounds **2** indicating an enhanced ICT.

The photophysical properties of compounds **1** and **2** were measured in a series of aprotic solvents of various polarity, estimated by the Dimroth-Reichardt parameter.[16] Concerning the absorption spectra (see Table S1), a bathochromic shift is observed in chlorinated solvents (CH_2Cl_2 and $CHCl_3$) indicating that the excited state of the studied chromophore can be effectively stabilized by polarizable halogentated solvent.[17] For compounds **1b**, **1c** and **2b**, a bathochromic shift attributed to the formation of J-aggregate[18] is also observed in heptane. The results of emission solvatochromism are given in Table 2. As observed generally for push-pull compounds,[7a,8b-c,11b-c,19] the studied chromophores showed a significant positive emission solvatochromism. This solvatochromic behavior results from the stabilization of the highly polar emitting state by polar solvents.[20] As examples, the PL spectra and the color changes observed upon UV-irradiation of compound **1a** in various solvents are shown in Figures 2-3 and S4. It should be noted that intense luminescence is only observed in chlorinated solvents ($CHCl_3$ and CH_2Cl_2) and in THF.

Table 2 Emission solvatochromism of TPA derivatives **1**–**7** in various aprotic solvents.

	Heptane	Toluene	1,4-dioxane	THF	CH_2Cl_2	Acetone
	30.9[a]	33.9[a]	36.0[a]	37.4[a]	40.7[a]	42.2[a]
Compd	λ_{max} (nm)	λ_{max} (nm)	λ_{max} (nm)	λ_{max} (nm)	λ_{max} (nm)	λ_{max} (nm)
1a	544	574	591	628	661	676
1b	679	568	587	634	645	688
1c	-	566	593	630	643	-
2a	573	611	618	663	686	-
2b	570	607	627	667	677	-

[a] $E_T(30)$, Dimroth–Reichardt polarity parameter in kcal mol^{-1}.

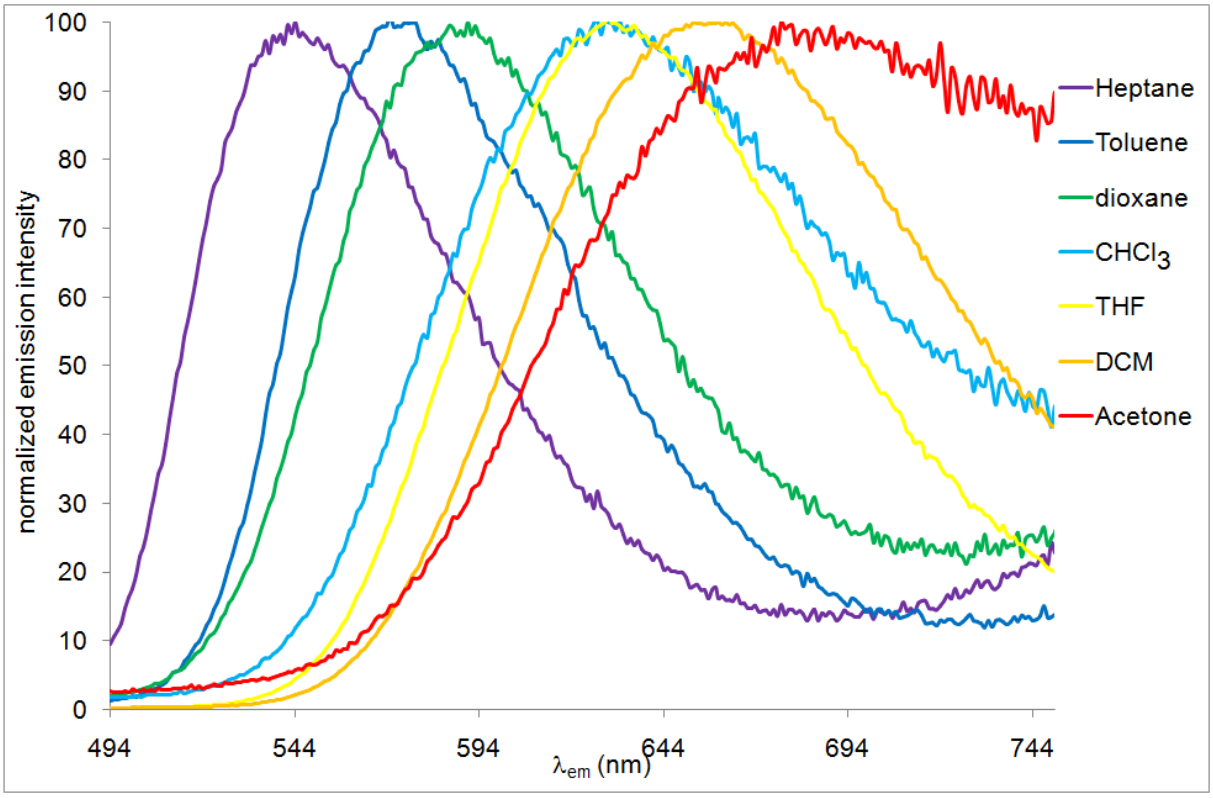

Figure 2: Normalized emission spectra of compound **1a** in various solvents.

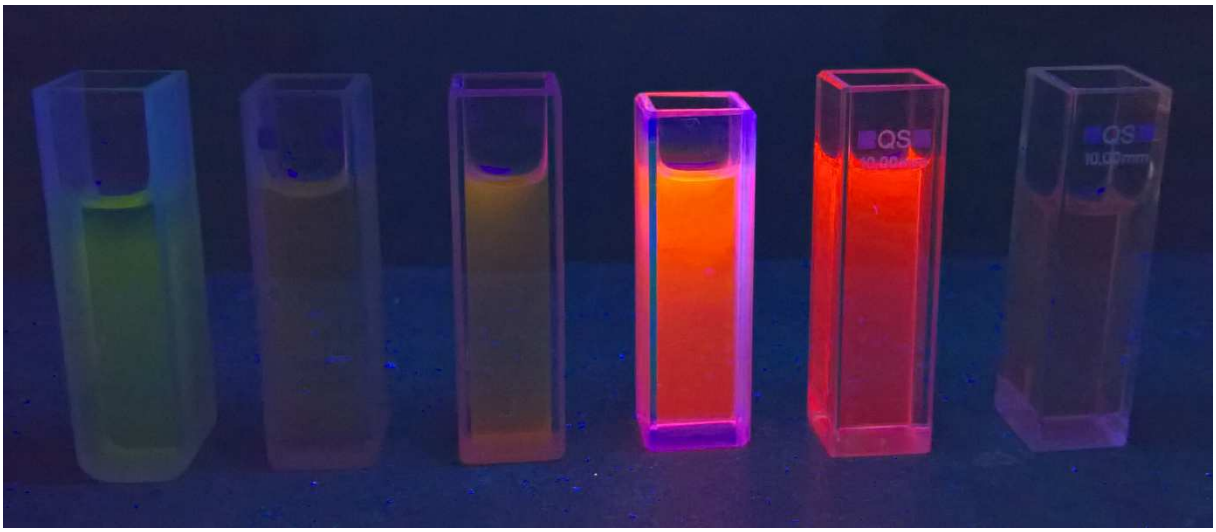

Figure 3: Fluorescence color change of **1a** in various solvents (from left to right: heptane, toluene, 1,4-dioxane, $CHCl_3$, CH_2Cl_2, Acetone) with a hand-held UV lamp (λ_{exc} = 366 nm).

Due to the presence of protonable amino groups in the structure of compounds **1**, the effect of progressive addition of camphorsulphonic acid (CSA) on the photophysical properties of compound **1a** has been studied. The addition of CSA (10^{-2} M), in chloroform solution of compound **1a** lead to a red-shifted absorption (λ_{abs} = 512 nm) and emission (λ_{em} = 672 nm) maxima with an increased fluorescence quantum yield (Φ_F =0.20) (Figure 4)

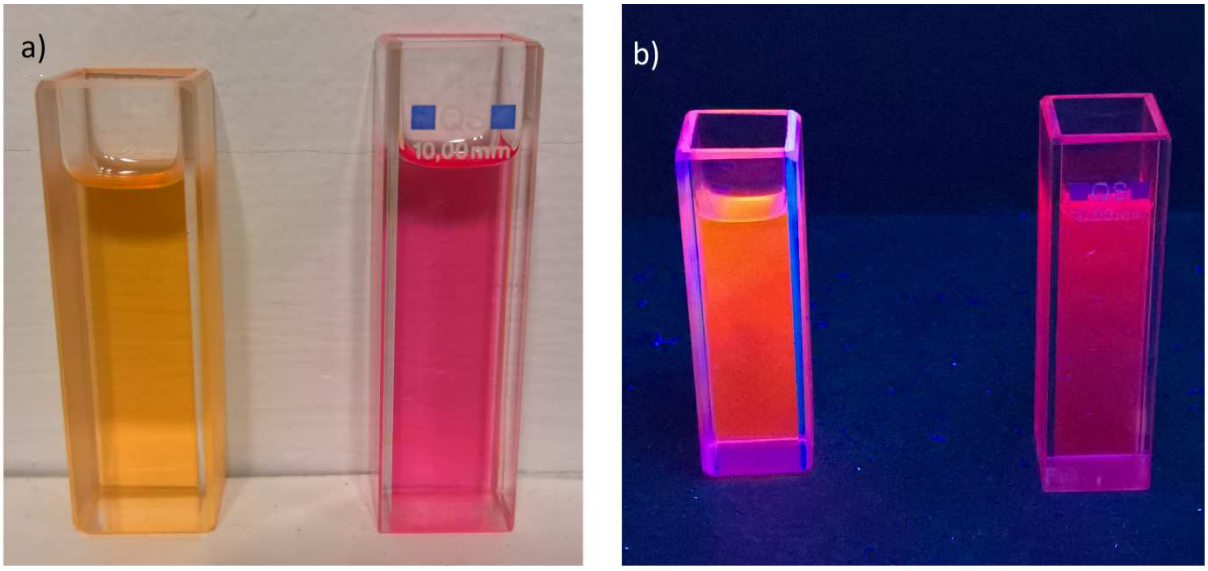

Figure **4**: Color change of $CHCl_3$ solution of **1a** without (left) or with (right) the addition of CSA (10^{-2} M) under white light (part a) or UV lamp irradiation (λ_{exc} = 366 nm).

The evolution of the emission spectrum of chloroform solution of compound **1a** upon progressive addition of CSA is shown on Figure 5. Contrary to what is observed generally in case of an acid-base equilibrium, no isobestic point is shown. The progressive bathochromic shift of the emission band might be attributed to a polarity and ionic strength increase of the media instead of the protonation of the chromophore.

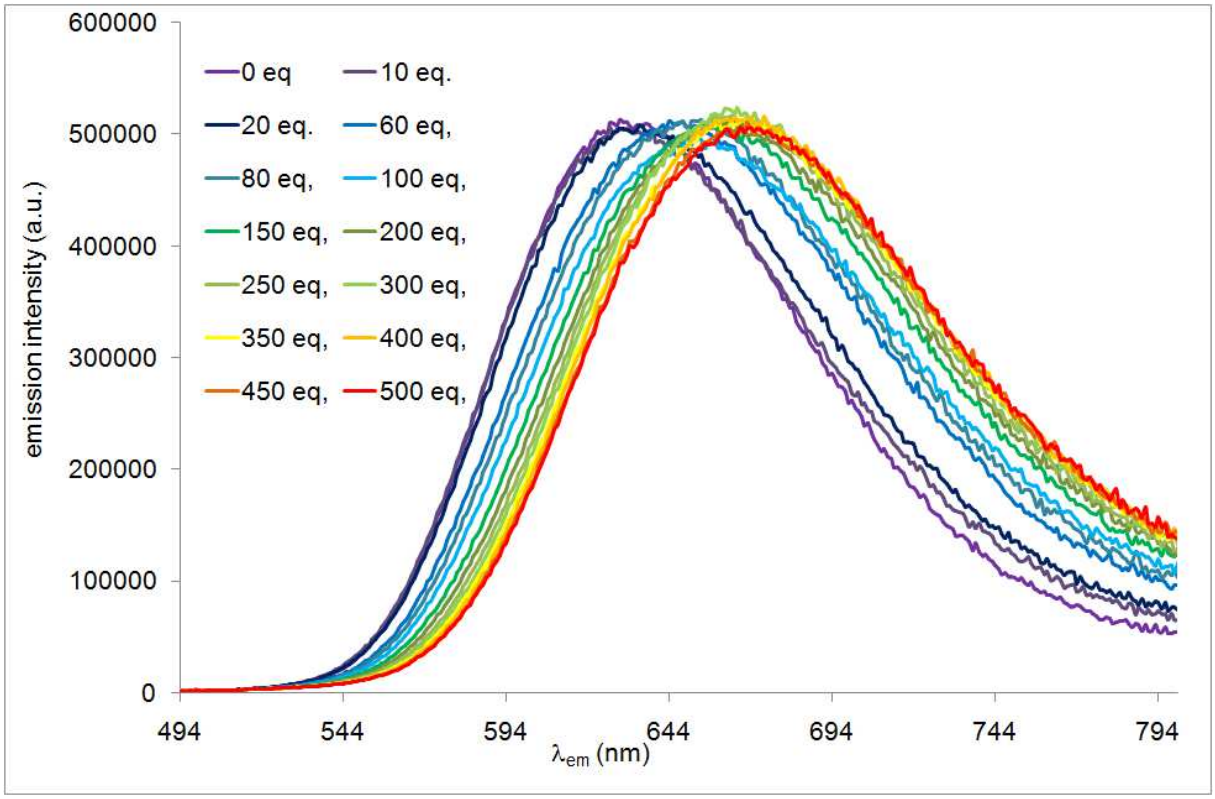

Figure 5: Change in the emission spectra of a $CHCl_3$ solution of **1a** (c = 2.0 × 10^{-5} M) upon addition of CSA

Second Order NLO properties

The second-order NLO responses of chromophores **1** and **2** were measured by the EFISH technique in $CHCl_3$ solution with a non resonant incident wavelength of 1907 nm. The second harmonic at λ = 953 nm stays well clear of the absorption bands of the chromophores.

Experimental details on EFISH measurements are given elsewhere.[21] EFISH measurements provide information about the scalar product $\mu\beta$ (2ω) of the vector component of the first hyperpolarisability tensor β and the dipole moment vector.[22] This product is derived according to equation 1 and considering γ_0(-2ω,ω,ω,0), the third-order term, as negligible for the push-pull compounds under consideration. This approximation is usually used for push-pull organic molecules.

$$\gamma_{EFISH} = \mu\beta/5kT + \gamma_0(-2\omega,\omega,\omega,0) \qquad \text{Eq. 1}$$

The results of EFISH measurements are presented in Table 3. For all the compounds, positive $\mu\beta$ were obtained, indicating that excited states are more polarized than the ground state and that both ground and excited states are polarized in the same direction. Compounds **1** and **2** exhibited higher NLO response than Disperse Red 1 generally used as reference ($\mu\beta$ = 450 10^{-48} esu).[23] Coumarin derivatives **2** exhibit higher NLO response than their aniline analogues. In the aniline series, the multisubstitution of the triphenylamine core leading to the quadrupolar structure **1b** and the octupolar structure **1c** results in a reduction of the NLO response with regard to the dipolar monosubstituted triphenylamine derivative **1a**. Even if the $\mu\beta$ value of chromophore **2b** is higher than that of **2a**, its figure of merit is significantly lower.

Table 3. Results of EFISH measurements for compounds **1** and **2.**

	1a	**1b**	**1c**	**2a**	**2b**
$\mu\beta$ [10^{-48} esu][a]	880	770	670	1400	1750
$\mu\beta_0$ [10^{-48} esu][b]	600	510	450	930	1240
$\mu\beta$/MW[c]	2.0	1.2	0.8	2.5	2.0

[a] $\mu\beta$ (2ω) at 1907 nm in $CHCl_3$. Molecular concentrations used for the measurements were in the range 10^{-3} to 10^{-2} M. $\mu\beta$ ± 10% [b] Two level corrected β values (β_0).[24] [c] Figure of merit 10^{-48} esu g mol^{-1}

Thermal properties

The thermal stability of NLO chromophores is also a key parameter for application in devices due to the high temperature requested for preparation processes. Thermogravimetric analysis

(TGA) for compounds **1a**, **1b** and **2** (Figure 6) showed good stability with thermal decomposition occurring at temperature higher to 300°C which is sufficiently high for application in electro-optical device application. Compounds **1c** and **2b** showed thermal decomposition beginning at lower temperature (around 250°C)

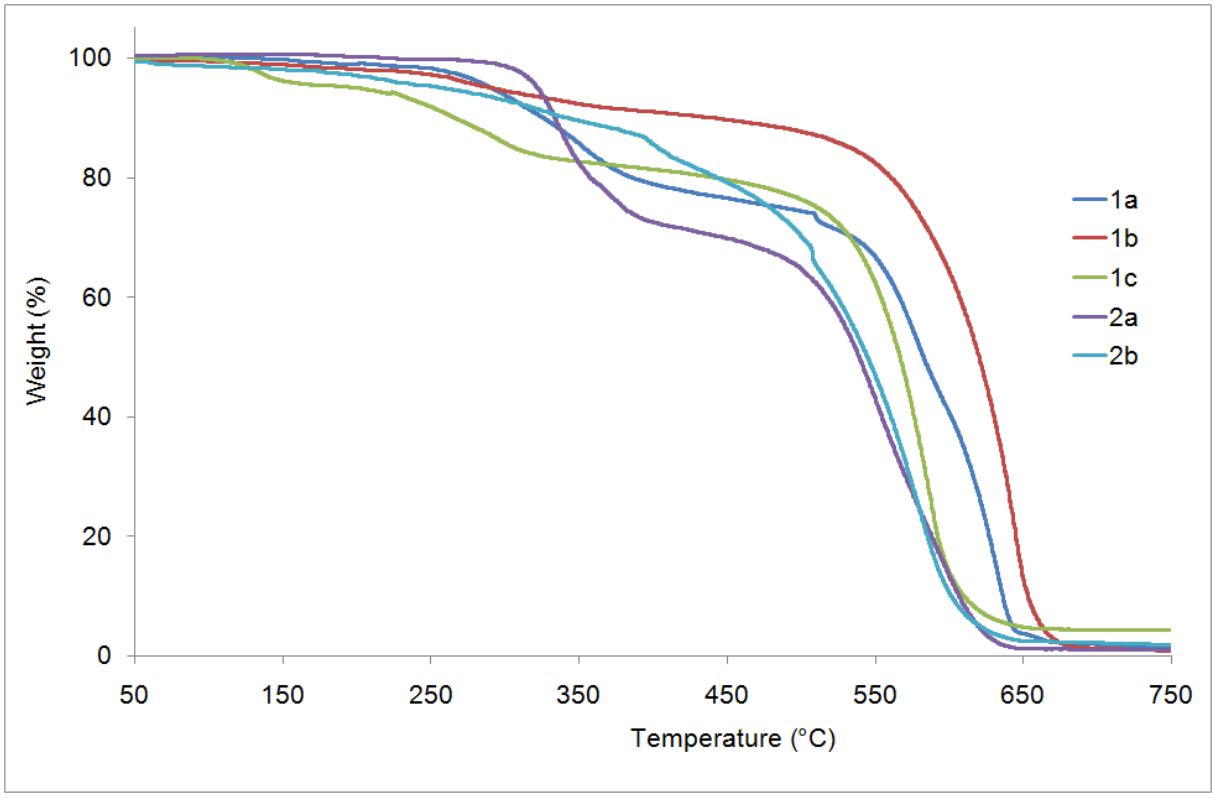

Figure 6: TGA curves of chromophores **1** and **2**

Computational studies

The optimized structures of the compound **1** and **2** in $CHCl_3$ are shown in Figure 7 and S1-S4. The selected geometrical parameters are given in Table S1. Ground state geometries of studied molecules showed that the π-conjugated linker between the diphenylamino group and the cyano fragments were not completely planar, with out-of-plane twist angles of less than 25° which increases in the following order **1a** (17.8°) < **1b** (20.2°, 21.5°) < **1c** (23.7°, 23.8°, 24.3°) and **2a** (11.7°) < **2b** (16.0°, 16.2°). Moreover the Bound length alternation (BLA) has been calculated for the vinylic linker of each branch of the chromophores. The results are provided in table 4. BLA value increases in the following order: **1a** < **1b** < **1c** and **2a** < **2b**.

These results indicates that the ICT decreases upon multisubstitution of the triphenylamine core and that the coumarin fragment, with respect to the aniline one, significantly enhances ICT into the chromophores, in accordance experimental NLO response.

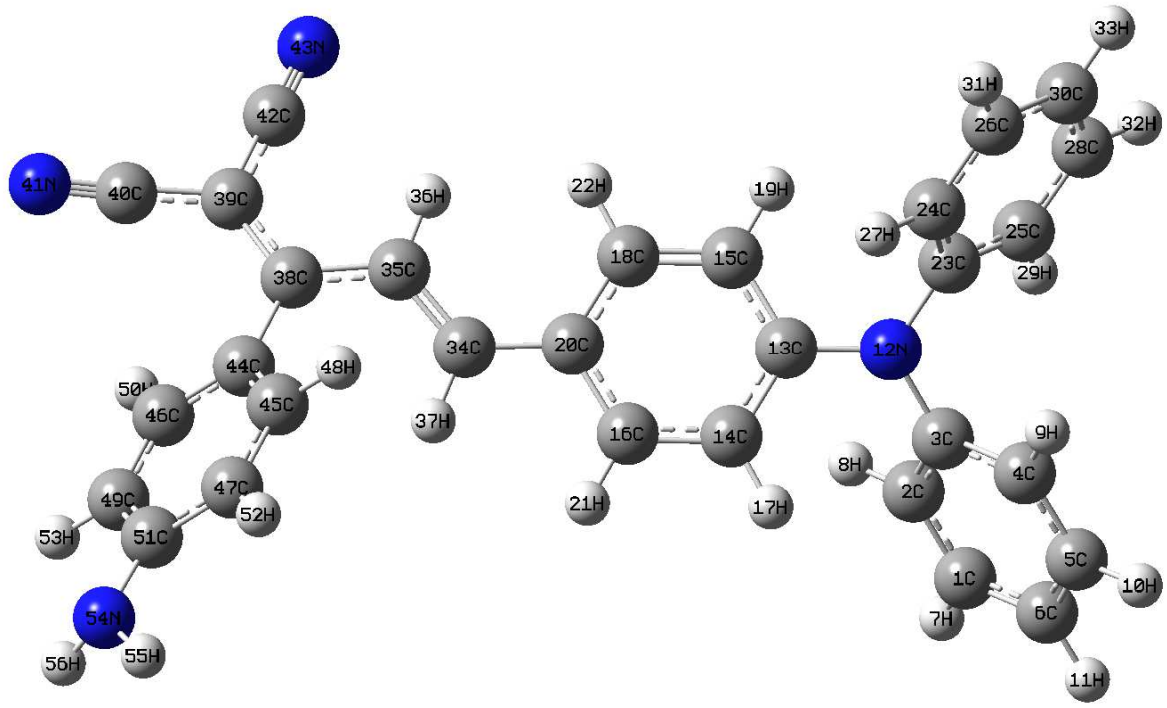

Figure 7. Optimized structure of **1a** in ground state.

Table 4. BLA in (Å) calculated for the vinylic linker on each branch of chromophores **1** and **2**.

	1st branch	2nd branch	3rd branch
1a	0.06287	-	-
1b	0.06948	0.06907	-
1c	0.0732	0.0727	0.07266
2a	0.05875	-	-
2b	0.06624	0.06619	-

To get further information about electronic structures of all studied molecules, TD-DFT calculations were performed with cam-B3LYP/6-31+g(d,p) in $CHCl_3$. Calculated absorption maxima, oscillator strengths and the contributions of orbital transitions for compounds 1 and 2 are given in Table 5. As seen from the table, the major contributions for main absorption band come from the transition HOMO→LUMO (83-88%). Apart from a systematic blue shift of the TD-DFT results with respect to the experimental ones, similar trends are observed: a red-shift of absorption maxima for polysubstituted triphenylamines. HOMO, LUMO energies and the energy gap between HOMO and LUMO (ΔE) are also provided in Table 5. The calculations show that ΔE value changes in order to **1a** > **1b** ~ **1c** and **2a** > **2b,** in accordance with experimental absorption maxima but in contradiction with BLA calculations.

Table 5. TD-DFT Computed UV-vis data for compounds **1** and **2**.

Molecules	$\lambda_{max}^{cal.}$	***f***	**Transitions**	**Contributions (%)**	E_{HOMO} **(eV)**	E_{LUMO} **(eV)**	**ΔE (eV)**
1a	439	1.4412	HOMO→LUMO	88	-5.25	-2.56	2.69
			HOMO-2→LUMO	6			
1b	459	1.8814	HOMO→LUMO	83	-5.36	-2.80	2.56
			HOMO-3→LUMO+1	10			
			HOMO→LUMO+2	3			
1c	445	1.6600	HOMO→LUMO	80	-5.44	-2.86	2.58
			HOMO-5→LUMO+1	2			
			HOMO-5→LUMO+2	6			
			HOMO-4→LUMO	2			
2a	458	1.4987	HOMO→LUMO	85	-5.24	-2.68	2.57
			HOMO-2→LUMO	5			
			HOMO-1→LUMO	3			
2b	468	2.0322	HOMO→LUMO	80	-5.34	-2.90	2.44
			HOMO-3→LUMO+1	9			

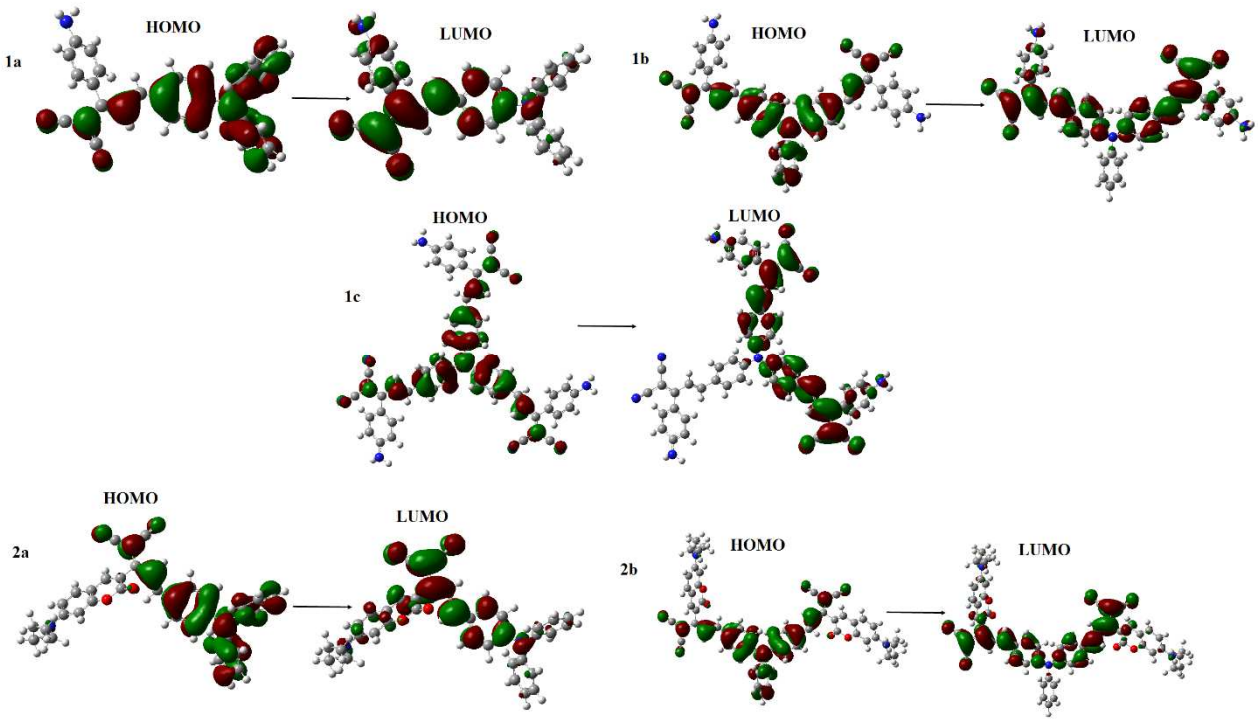

Figure 8. HOMO and LUMO localizations in **1a-1c** and **2a-2b**.

As shown on Figure 8, the HOMOs are localized on the donating triphenylamine moiety while the LUMOs are localized dicyanomethylene acceptor groups for all the studied compounds. However, for compound **1c**, the LUMO occupies only two branches, the third one being completely vacant indicating that there is no contribution to the charge transitions from that branch. This is a common feature of tripodal triphenylamine push-pull chromophores.[7a,8a,20a]

The calculated electrical dipole moment (μ) and first hyperpolarizability (β) values at B3LYP/6-311++g(2d,p) in chloroform are given in Table 6. The calculations indicate a decrease of the β values from **1a** to **1c** and from **2a** to **2b**. For compounds **2**, the presence of the coumarin fragment in the structure provided an increase in the NLO property with respect to compounds **1** in accordance with experimental results.

Table 6. Calculated electrical dipole moment (μ) and first hyperpolarizability (β) values of compounds **1** and **2** at B3LYP/6-311++g(2d,p) in chloroform.

	μ (D)	β ($\times 10^{-24}$ esu)
1a	15.0	576
1b	13.7	527
1c	9.6	99
2a	15.2	649
2b	22.0	625

Conclusion

In summary**,** five chromophores with a triphenylamine core and analine/coumarin decorated allylidenemalonitrile fragments have been synthesized. Their photophysical properties have been measured. These compounds exhibit strong emission in chlorinated solvent and the intense emission solvatochromism observed is characteristic of a strong ICT. Relatively high NLO response ($\mu\beta$) have been obtained and the following trends have been observed: the multisubstitution of the triphenylamine core results in a decrease of the figure of merit and coumarin fragments on allylidenemalonitrile significantly enhance the NLO response with respect to their aniline analogues. The easy synthesis, high thermal stability and important figure of merit of chromophores **1a** and **2a** make them interesting candidate to be incorporated into polymeric films for second harmonic generation.

Experimental section

Materials

All chemicals were purchased from commercial sources and were used without further purification. 2-(1-(4-aminophenyl)ethylidene)malononitrile and 2-(1-(7-(diethylamino)-2-oxo-2H-chromen-3-yl)ethylidene)malononitrile were obtained as described in the literature.[14]

Thin-layer chromatography (TLC) was used for monitoring the domino reactions using precoated silica gel 60 F254 plates. $^{1}H/^{13}C$ NMR spectra were recorded on NMR spectrometer Bruker-Spectrospin Avance DPX 300 and Ultra-Shield in DMSO-d_6. Chemical shifts (δ) are given in parts per million (ppm) using the residue solvent peaks as reference relative to TMS. Coupling constants (J) are given in hertz (Hz). High resolution mass spectra (HRMS) were recorded at Gazi University Faculty of Pharmacy using electron ionization (EI) mass spectrometry (Waters-LCT-Premier-XE-LTOF (TOF-MS) instruments; in m/z (rel. %). FT-IR spectra were recorded on Nicolet iS5 FT-IR Spectrometer equipped with ATR system. The melting points were measured using Electrothermal IA9200 apparatus. Absorbance and emission spectra were recorded by using a Spex FluoroMax-3 Jobin–Yvon Horiba spectrofluorimeter. Compounds were excited at their absorption maxima (longest-wavelength absorption band) to record the emission spectra. The Φ_F values were calculated by using a well-known procedure with 9,10-bis(phenylethynyl)anthracene in cyclohexane as standard.[25] Stokes shifts were calculated by considering the lowest-energy absorption band.

Computational methods

The calculations were performed using Gaussian 09 package program.[26] The compounds were optimized using Density Functional Theory (DFT) at B3LYP/631g(d) level.[27] The vibrational analysis verify that the optimized structures correspond to local minima on the energy surface. The time-dependent density functional theory (TD-DFT) calculations were performed at cam-B3LYP/631+g(d,p) level. To obtain the second order NLO properties of the molecules, the dipole moment (μ) and hyperpolarizability (β) were estimated from the calculations performed using B3LYP/6311+g(2d,p) level. All calculations were done in $CHCl_3$ with the polarized continuum model (PCM) [4].[28]

*General procedure for the synthesis of compounds **1a-b** and **2a-b***

A mixture of the corresponding triphenylamine carboxaldehyde (2 mmol) and the appropriate ethylidenemalononitrile (1.4 eq per formyl group) and a few drops piperidine in 40 mL ethanol was stirred under reflux untill completion of the reaction (8-48 h). After cooling to room temperature the precipitate was filltered off and then recrystallized from ethanol.

(E)-2-(1-(4-aminophenyl)-3-(4-(diphenylamino)phenyl)allylidene)malononitrile ***(1a)*** *:* Red solid. Yield: 74% (649 mg) mp: 205-207 ^{o}C FT-IR (cm^{-1}): 3456-3361 (NH_2), 3036 (CH ar), 2217 (CN), 1626-1600 (CC ar) 1581 (CC ar). ^{1}H-NMR (DMSO-d_6, δ): 7.58 (d, *J* = 8.8 Hz, 2H), 7.38-7.16 (m, 13 H), 7.00 (d, *J* = 15.3 Hz, 1H), 6.87 (d, *J* = 8.6 Hz, 2H), 6.67 (d, *J* = 8.5 Hz, 2H), 6.13 (s, 2H). ^{13}C-NMR (DMSO-d_6 , δ): 171.4, 153.6, 150.7, 148.3, 146.4, 132.5, 130.9, 130.3, 127.6, 126.1, 125.3, 122.2, 120.6, 119.9, 116.4, 115.5, 113.6, 73.1. HR-MS (*m*/z), $[M+H]^+$: $C_{30}H_{23}N_4$, calculated: 439.1917; found: 439.1935

2,2'-((2E,2'E)-((phenylazanediyl)bis(4,1-phenylene))bis(1-(4-aminophenyl)prop-2-en-3-yl-1-ylidene))dimalononitrile ***(1b)*** : Red solid. Yield: 70% (886 mg) mp: 248-250 ^{o}C FT-IR (cm^{-1}): 3487-3375 (NH_2), 3336 (NH), 2592 (CN), 1600 (CC ar) ^{1}H-NMR (DMSO-d_6, δ): 7.66 (d, *J* = 8.6 Hz, 4H), 7.45 – 6.95 (m, 17H), 6.68 (d, *J* = 8.6 Hz, 4H), 6.17 (s, 4H). ^{13}C-NMR (DMSO-d_6 , δ): 171.1, 153.7, 149.3, 147.7, 145.8, 132.6, 130.9, 130.5, 129.6, 126.7, 126.1, 123.4, 119.7, 116.3, 115.4, 113.6, 73,6. HR-MS (*m*/z) , $[M+H]^+$: $C_{42}H_{30}N_7$, calculated: 632.2557 ; found: 632.2573

2,2',2''-((2E,2'E,2''E)-(nitrilotris(benzene-4,1-diyl))tris(1-(4-aminophenyl)prop-2-en-3-yl-1-ylidene))trimalononitrile ***(1c)*** : Tris(4-formylphenyl)amine (0.586 g, 0.71 mmol) and 2-(1-(4-aminophenyl)ethylidene)malononitrile (0.653 g, 3.57 mmol) were dissolved in absolute acetonitrile (40 mL). Piperidine was added in catalytic amount (0.1 mL) and the reaction mixture was refluxed under N_2 for 12 h. After cooling to r.t., the mixture was poured into ice-water and pH 7 with 1 M NaOH. The residue was chromatographed on a silica gel column

with ethyl acetate/n-hexane (v/v, 6/1) to produce of dark red solid. Yield: 40% (30 mg) mp: 180 ^{o}C FT-IR (cm^{-1}): 3471-3369 (NH_2), 2213 (CN), 1623 (CC ar), 1601 (CC ar). ^{1}H-NMR (DMSO-d_6, δ): 7.71 (d, *J* = 8.7 Hz, 6H), 7.36 (d, J = 15.6 Hz, 3H), 7.31 (d, *J* = 8.7 Hz, 6H), 7.12 (d, *J* = 8.7 Hz, 6H), 7.07 (d, *J* = 15.5 Hz, 3H), 6.68 (d, *J* = 8.7 Hz, 6H), 6.21 (s, 6H). ^{13}C-NMR (DMSO-d_6, δ): 171.1, 153.8, 148.6, 147.5, 132.7, 131.0, 124.9, 124.1, 119.7, 116.2, 115.4, 113.6, 74.0. HR-MS (*m*/z), $[M+H]^+$: $C_{54}H_{37}N_{10}$, calculated: 825.3197 ; found: 825.3225

*(E)-2-(1-(7-(diethylamino)-2-oxo-2H-chromen-3-yl)-3-(4-(diphenylamino)phenyl)allylidene)malononitrile (**2a**):* Red solid. Yield: 86% (970 mg) mp: 233-235 ^{o}C) FT-IR (cm^{-1}): 3062 (CH ar), 2967 (CH alk), 2222 (CN), 1706 (CO), 1622 (CC ar), 1579 (CC ar). ^{1}H-NMR (DMSO-d_6, δ): 8.08 (s, 1H), 7.63 (d, *J* = 8.7 Hz, 2H), 7.55 (d, *J* = 9.0 Hz, 1H), 7.43-7.13 (m, 12H), 6.85 (d, *J* = 8.7 Hz, 2H), 6.80 (dd, J_1 = 8.9 Hz, J_2 = 2.1 Hz, 1H), 6.64 (d, *J* = 1.5 Hz, 1H), 3.49 (q, *J* = 6.7 Hz, 4H), 1.15 (t, *J* = 6.9 Hz, 6H). ^{13}C-NMR (DMSO-d_6 , δ): 167.0, 158.7, 157.6, 152.5, 151.2, 148.9, 147.2, 146.2, 131.6, 130.4, 127.3, 126.4, 125.6, 120.6, 120.1, 114.8, 114.0, 112.4, 110.2, 107.8, 96.9, 78.7, 44.8, 12.8. HR-MS (*m*/z), $[M+H]^+$: $C_{37}H_{31}N_4O_2$ calculated: 563.2442 found: 563.2471.

*2,2'-((2E,2'E)-((phenylazanediyl)bis(4,1-phenylene))bis(1-(7-(diethylamino)-2-oxo-2H-chromen-3-yl)prop-2-en-3-yl-1-ylidene))dimalononitrile **(2b)** :* Black solid. Yield: 45% (792 mg) mp: 270-271 ^{o}C) FT-IR (cm^{-1}): 2929 (CH alk), 2216 (CN), 1714 (CO), 1615 (CC ar). ^{1}H-NMR (DMSO-d_6, δ): 8.10 (s, 2H), 7.71 (d, J = 8.7 Hz, 4H), 7.55 (d, *J* = 9.0 Hz, 2H), 7.46-7.14 (m, 7H), 7.05 (d, *J* = 8.6 Hz, 4H), 6.80 (dd, J_1 = 9.0 Hz, J_2 = 1.8 Hz, 4H), 6.65 (d, *J* = 1.8 Hz, 2H), 3.50 (q, *J* = 7.0 Hz, 8H), 1.15 (t, *J* = 6.9 Hz, 12H). Due du solubility problem, it was not possible to register a complete 13C nmr spectrum. HR-MS (*m*/z) , $[M+H]^+$: $C_{56}H_{46}N_7O_4$, calculated:880.3606 ; found: 880.3618.

Aknowledgements

The financial support of the The Scientific and Technological Research Council of Turkey (TUBITAK, Project no: 215Z567) is gratefully acknowledged. The numerical calculations reported in this paper were fully performed at TUBITAK ULAKBIM, High Performance and Grid Computing Center (TRUBA resources).

Conflicts of interest

There are no conflicts to declare.

[1] (a) T. Verbiest, K. Clays and V. Rodriguez, *Second-Oder Nonlinear Optical Characterization Techniques*, Eds CRC Press, Taylor & Francis Group, 2009; (b) R. W. Boyd, *Nonlinear Optics*, Eds Academic Press, 2003.

[2] (a) G. Thomas, J. van Voskuilen, H. C. Gerritsen and H. J. C. M. Sterenborg, *J. Photochem. Photobiol. B Biol.*, 2014, **141**, 128; (b) B. Weigelin, G. J. Bakker and P. Friedl, *J. Cell Sci.*, 2016, **129**, 245; (c) P.-J. Kim, J.-H. Jeong, M. Jazbinsek, S.-B. Choi, I.-H. Baek, J.-T. Kim, F. Rotermund, H. Yun, Y. S. Lee and P. Günter, *Adv. Funct. Mater.*, 2012, **22**, 200; (d) L. Meng, L. Zhang, Z. Hou, L. Wang, H. Xu, M. Shi, L. Wang, Y. Yang, Y. Qi, C. He, H. Yu, X. Lin, F. Su, M. Xia, R. Li, *Opt. Laser Technol.* 2018, *101*, 401.

[3] (a) S. R. Marder (guest ed.), Themed issue on Organic Nonlinear Optics, *J. Mater. Chem.*, 2009, **19**, 7381; (b) L. R. Dalton, P. A. Sullivan and D. H. Bale, *Chem. Rev.* 2010, **110**, 25; (c) B. J. Coe, *Coord. Chem. Rev.*, 2013, **257**, 1438; (d) E. Garmire, *Opt. Express*, 2013, **21**, 30532.

[4] (a) F. Bureš, *RSC Adv.* 2014, **4**, 58826; (b) C. Moreno-Yruela, J. Garín, S. Orduna, E. Quintero, J. T. López Navarrete, B. E. Diosdado, B. Villacampa, J. Casado, and R. Andreu, *J.*

Org. Chem. 2015, **80**, 12115; (c) P. Solanke, S. Achelle, N. Cabon, O. Pytela, A. Barsella, B. Caro, F. Robin-le Guen, J. Podlesny, M. Klikar and F. Bureš, *Dyes Pigm.*, 2016, **134**, 129.

[5] (a) F. Bureš, W. B. Schweizer, J. C. May, C. Boudon, J.-P. Gisselbrecht, M. Gross, I. Biaggio and F. Diederich, *Chem. Eur. J.*, 2007, **13**, 5378; (b) M. Klikar, F. Bureš, O. Pytela, T. Mikysek, Z. Padělková, A. Barsella, K. Dorkenoo and S. Achelle, *New. J. Chem.*, 2013, **37**, 4230; (c) Y. Wen, W. Wu, Y. Li, Y. Li, T. Qin, Y. Tang, L. Wang and J. Zhang, *Org. Electron.*, 2016, **38**, 61.

[6] M. Klikar, P. Solanke, J. Tydlitát and F. Bureš, *Chem. Rec.* 2016, **16**, 1886.

[7] (a) J. Tydlitát, S. Achelle, J. Rodríguez-López, O. Pytela, T. Mikýsek, N. Cabon, F. Robin-le Guen, D. Miklík, Z. Růžičková and F. Bureš, *Dyes Pigm.* 2017, **146**, 467; (b) V. Parthasarathy, S. Fery-forgues, E. Campioli, G. Recher, F. Terenziani and M. Blanchard-Desce, *Small* 2011, **7**, 3219; (c) H. Zhu, J. Huang, L. Kong, Y. Tian and J. Yang, *Dyes Pigm.* 2018, **151**, 140.

[8] (a) D. Cvejn, E. Michail, I. Polyzos, N. Almonasy, O. Pytela, M. Klikar, T. Mikysek, V. Giannetas, M. Fakis and F. Bureš, *J. Mater. Chem. C* **2015**, *3*, 7345; (b) D. Cvejn, S. Achelle, O. Pytela, J.-P. Malval, A. Spangenberg, N. Cabon, F. Bureš and F. Robin-le Guen, *Dyes Pigm.* 2016, **124**, 101; (c) C. Le Droumaguet, A. Soudron, E. Genin, O. Mongin and M. Blanchard-Desce, *Chem. Asian J.* 2013, **8**, 2984; (d) F. Hammerer, G. Garcia, S. Chen, F. Poyer, S. Achelle, C. Fiorini-Debuisschert, M.-P. Teulade-Fichou and P. Maillard, *J. Org. Chem.* 2014, **79**, 2337; (e) B. Dumat, G. Bordeau, E. Faurel-Paul, F. Mahuteau-Betzer, N. Saettel, G. Metge, C. Fiorini-Debuisschert, F. Charra and M.-P. Teulade-Fichou, *J. Am. Chem. Soc.* 2013, **135**, 12697.

[9] (a) C. Katan, S. Tretiak, M. H. V. Werts, A. J. Bain, R. J. Marsh, N. Leonczek, N. Nicolaou, E. Badaeva, O. Mongin and M. Blanchard-Desce, *J. Phys. Chem. B* 2007, **111**, 9468; (b) D. Cvejn, E. Michail, K. Seintis, M. Klikar, O. Pytela, T. Mikysek, N. Amonasy, M. Ludwig, V.

Giannetas, M. Fakis and F. Bureš, *RSC Adv.* 2016, *6*, 12819; (c) M. Klikar, K. Seintis, I. Polyzos, O. Pytela, T. Mikysek, N. Almonasy, M. Fakis and F. Bureš, ChemPhotoChem doi: 10.1002/cptc.201800051

[10] (a) J. Wu, B. A. Wilson, D. W. Smith Jr and S. O. Nielsen, *J. Mater. Chem. C* 2014, **2**, 2591; (b) F. Liu, Y. Yang, H. Wang, J. Liu, C. Hu, F. Huo, S. Bo, Z. Zhen, X. Liu and L. Qiu, *Dyes Pigm.* 2015, **120**, 347; (c) M. Klikar, P. le Poul, A. Růžička, O. Pytela, A. Barsella, K. D. Dorkenoo, F. Robin-le Guen, F. Bureš, and S. Achelle, *J. Org. Chem.* 2017, **82**, 9435;

[11] (a) Z. Li, P. Chen, Z. Li and J. Qin, *Adv. Electronic Mater.* 2017, **3**, 1700138; (b) R. D. Fonseca, M. G. Vivas, D. L. Silva, G. Eucat, Y. Bretonnière, C. Andraud, L. De Boni and C. R. Mendonça, *J. Phys. Chem. C* 2018, **122**, 1770; (c) Y. Erande, S. Kothavale, M. C. Sreenath, S. Chitrambalam, I. H. Joe and N. Sekar, *Dyes Pigm.* 2018, **148**, 474.

[12] (a) U. Warde and N. Sekar, *J. Fluoresc.* 2018, **28**, 293; (b) N. Seferoğlu, Y. Bayrak, E. Yalçın and Z. Seferoğlu, *J. Mol. Struct.* 2017, **1149**, 510.

[13] E. Yalçın, S. Achelle, Y. Bayrak, N. Seferoğlu, A. Barsella and Z. Seferoğlu, *Tetrahedron Lett.* 2015, **56**, 2586.

[14] B. Aydıner, E. Yalçın, V. Korkmaz and Z. Seferoğlu, *Synth Commun.* 2017, **47**, 2174.

[15] (a) S. Easwaramoorthi, P. Thamaraiselvi, K. Duraimurugan, A. J. Beneto, A. Siva and B. U. Nair, *Chem. Commun.*, 2014, **50**, 6902; (b) J. Weng, Q. Mei, Q. Fan, Q. Ling, B. Tong, W. Huang, *RSC Adv.* 2013, **3**, 21877.

[16] C. Reichardt, *Chem. Rev.* 1994, **94**, 2319.

[17] S. Achelle, S. Khlal, A. Barsella, J.-Y. Saillard, X. Che, J. Vallet, F. Bureš, B. Caro and F. Robin-le Guen, *Dyes Pigm.* 2015, **113**, 562.

[18] S. Gadde, E. K. Batchelor, J. P. Weiss, Y. Ling and A. Kaifer, *J. Am. Chem. Soc.* 2008, **130**, 17114.

[19] (a) K. Hoffert, R. J. Durand, S. Gauthier, F. Robin-le Guen, S. Achelle, *Eur. J. Org. Chem.* 2017, 523; (b) C. Denneval, S. Achelle, C. Baudequin and F. Robin-le Guen, *Dyes Pigm.* 2014, **110**, 49.

[20] (a) C. Katan, F. Terenziani, O. Mongin, M. H. W. Wertz, L. Porrès, T. Pons, J. Mertz, S. Tretiak and M. Blanchard-Desce, *J. Phys. Chem. A* 2005, **109**, 3024; (b) R. Lartia, C. Allain, G. Bordeau, F. Schmidt, C. Fiorini-Debuisschert, F. Charra and M.-P. Teulade-Fichou, *J. Org. Chem.* 2008, **73**, 1732.

[21] G. Ulrich, A. Barsella, A. Boeglin, S. Niu, and R. Ziessel, *ChemPhysChem.*, 2014, **15**, 2693.

[22] (a) K. D. Singer and A. F. Garito, *J. Phys. Chem.* **1981**, *75*, 3572; (b) B. F. Levine and C. G. Bethea, *Appl. Phys. Lett.* **1974**, *24*, 445; (c) I. Ledoux and J. Zyss, *Chem. Phys.* **1982**, *73*, 203; (d) T. Thami, P. Bassoul, M. A. Petit, J. Simon, A. Fort, M. Barzoukas and A. Villaeys, *J. Am. Chem. Soc.* **1992**, *114*, 915.

[23] S. Di Bella, C. Dragometti, M. Pizzotti, D. Roberto, F. Tessore, R. Uno, In: H. Le Bozec and V. Guerchais editors. Topics in Organometallic Chemistry vol 28: Molecular Organometallic Mateirals for Optics, Springer Verlag Berlin Heidelberg 2010, p. 1-57.

[24] C. E. Powell and M. G. Humphrey, *Coord. Chem. Rev.* 2004, **248**, 725.

[25] D. F. Eaton, *Pure Appl. Chem.* 1988, **60**, 1107.

[26] M. J. Frisch, G. W. Trucks, H. B. Schlegel, G. E. Scuseria, M. A. Robb, J. R. Cheeseman, G. Scalmani, V. Barone, B. Mennucci, G. A. Petersson, H. Nakatsuji, M. Caricato, X. Li, H. P. Hratchian, A. F. Izmaylov, J. Bloino, G. Zheng, J. L. Sonnenberg, M. Hada, M. Ehara, K. Toyota, R. Fukuda, J. Hasegawa, M. Ishida, T. Nakajima, Y. Honda, O. Kitao, H. Nakai, T. Vreven, J. A. Jr Montgomery, J. E. Peralta, F. Ogliaro, M. Bearpark, J. J. Heyd, E. Brothers, K. N. Kudin, V. N. Staroverov, R. Kobayashi, J. Normand, K. Raghavachari, A. Rendell, J. C. Burant, S. S. Iyengar, J. Tomasi, M. Cossi, N. Rega, J. M. Millam, M. Klene, J. E. Knox, J. B.

Cross, V. Bakken, C. Adamo, J. Jaramillo, R. Gomperts, R. E. Stratmann, O. Yazyev, A. J. Austin, R. Cammi, C. Pomelli, J. W. Ochterski, R. L. Martin, K. Morokuma, V. G. Zakrzewski, G. A. Voth, P. Salvador, J. J. Dannenberg, S. Dapprich, A. D. Daniels, E. O. Farkas, J. B. Foresman, J. V. Ortiz, J. Cioslowski, D. J. Fox, Gaussian 09, Revision C.01; Gaussian: Wallingford, CT, 2009.

[27] (a) W. Kohn, L. J. Sham, *Phys. Rev.* 1965, **140**, A1133; (b) A. D. Becke, *J. Chem. Phys.* 1993, **98**, 5648.

[28] (a) J. Tomasi, R. Cammi, B. Mennucci, C. Cappelli, S. Corni, *Phys. Chem. Chem. Phys.* 2002, **24**, 5697; (b) M. Cossi and V. Barone, *J. Chem. Phys.* 2001, **115**, 4708.